Received: 2 June 2020 | Revised: 30 July 2020 | Accepted: 5 August 2020

DOI: 10.1002/aoc.6004

Applied Organometallic Chemistry WILEY

FULL PAPER

Sulfonic acid-functionalized Fe_3O_4-supported magnetized graphene oxide quantum dots: A novel organic-inorganic nanocomposite as an efficient and recyclable nanocatalyst for the synthesis of dihydropyrano[2,3-*c*]pyrazole and 4*H*-chromene derivatives

Masoud Khaleghi Abbasabadi[1] | **Davood Azarifar**[1] | **Hamid Reza Esmaili Zand**[2]

[1]Department of Chemistry, Bu-Ali Sina University, Hamedan, 65178, Iran

[2]Department of Chemistry, Iran University of Science and Technology, Tehran, Iran

Correspondence
Masoud Khaleghi Abbasabadi, Department of Chemistry, Bu-Ali Sina University, 65178, Hamedan, Iran.
Email: m.khaleghi@alumni.basu.ac.ir

In this research, the main emphasis has been focused on the preparation of a novel Fe_3O_4-supported propane-1-sulfonic acid-grafted graphene oxide quantum dots (Fe_3O_4@GOQD-*O*-(propane-1-sulfonic acid)) that it was readily synthesized via a five-step procedure as a hitherto unreported magnetic nanocatalyst. This newly prepared Fe_3O_4@GOQD-*O*-(propane-1-sulfonic acid) nanocomposite was structurally well-established by different analytical techniques including Fourier transform infrared (FT-IR), X-ray diffraction (XRD), energy-dispersive X-ray (EDX), thermal gravimetric analysis (TGA), field emission gun-scanning electron microscope (FESEM), high-resolution transmission electron microscopy (HRTEM) and vibrating sample magnetometer (VSM) analyses. The high catalytic performance of this nanocomposite was exhibited in one-pot synthesis of dihydropyrano[2,3-*c*]pyrazole and 4*H*-chromene derivatives under mild conditions. Low reaction times, excellent yields of the products, benignity of the catalyst, easy reaction work-up and magnetic recyclability of the catalyst are the main advantages of the present protocol. Also, our research indicated that the Fe_3O_4@GOQD-*O*-(propane-1-sulfonic acid) could be reused up to five times without considerable loss of catalytic activity.

KEYWORDS

4*H*-chromene, dihydropyrano[2,3-*c*]pyrazoles, Fe_3O_4-supported propane-1-sulfonic acid-grafted graphene oxide quantum dot, nanocomposite, one-pot three-component reaction

1 | INTRODUCTION

In recent decade, heterogeneous catalysts have found a wide range of applications as eco-friendly and compatible catalysts in several synthetic reactions and industrial fields.[1–4] In the past decade, several studies have been directed on the preparation and application of various magnetic nanoparticles (MNPs) in different fields such as the biological and pharmaceutical industry, magnetic resonance imaging, bioseparation, hyperthermia and catalytic processes. Also, MNPs have attracted much research interests as highly active supports for preparation of various supported nanocatalysts which can be easily separated from the mixture reaction simply by using an external magnetic field.[5] Among the heterogeneous catalysts, several nanoparticles (NPs) have

received great interest due to their high catalytic activity and interesting physical and chemical properties such as nontoxicity, reusability, long-term stability and high surface area.[6] Despite these advantages, such small particles suffer from tedious recycling and separation from the reaction mixtures by filtration or expensive ultracentrifugation that has limited their application.[7] This drawback has been tackled by using MNPs as efficient supports amenable to simple magnetic separation.[8] As a result, MNPs have found wide applications in catalytic organic reactions and industrial processes.[9,10] In this context, Fe_3O_4 and Fe_2O_3 NPs are the most extensively studied core magnetic supports, owing to their high surface area with high catalyst loading ability, magnetic susceptibility, conductivity, striking stability and catalytic activity.[11]

Among the NPs known in the recent years, carbon nanostructured materials have attracted enormous interest as efficient catalysts in different chemical processes due to their interesting properties such as air stability, low cost and high corrosion resistance.[12] Graphitic materials have emerged as the most widely used carbon materials in various fields owing to their appropriate electrical conductivity, high mechanical strength, suitable transparency, high surface area and proper biocompatibility.[13] Graphene oxide (GO) has been reported to possess oxidative catalytic activity and emerged as an air-stable eco-friendly heterogeneous catalyst and easily functionalized catalyst for applications in various chemical reactions.[14,15] GO is built of layers of six-membered aromatic rings carrying various functional groups such as hydroxyl, carboxyl and epoxy groups. Such functional groups enable the carbon layers of GO to mediate ionic and non-ionic interactions with a wide range of molecules and also to perform oxidizing and acidic activities in different reactions.[14] Among the carbon nanomaterials, graphene quantum dots (GQDs) have been known as a new class of compounds consisting a single atomic layer of nanosized graphene unit.[14,15] In recent years, GQDs have received enormous research interest owing to its excellent structural features including easy functionalization, low toxicity, excellent solubility, high surface area, excellent thermal and chemical stability, biocompatibility and stable photoluminescence.[16]

Among the heterocyclic compounds of the biological activities, 4*H*-pyrane-containing derivatives have emerged as an important class of heterocyclic compounds with diverse biological activities. Pyrano[2,3-*c*]pyrazole derivatives have received considerable interest owing to their significant pharmacological and therapeutic values as antibacterial, anticoagulant, anticancer, diuretic and insecticidal agents.[17,18] Besides, these compounds constitute the structural unit for the synthesis of some promising drugs, pharmaceutical agents and photoactive materials.[18–21]

The general synthesis of dihydropyrano[2,3-*c*]pyrazole derivatives involves three-component condensation reactions between malononitrile, 3-methyl-1-phenyl-pyrazolin-5-one and aldehydes under the catalytic effect of various catalytic systems such as piperidine, hexadecyldimethylbenzyl ammonium bromide (HDMBAB), MgO, γ-Fe_2O_3@Cu_3Al-LDH, ionic liquids and cupreine.[22]

Similarly, 4*H*-chromene derivatives have found to exhibit intriguing pharmaceutical properties as hypotensive, antimicrobial, antitumor, antileishmanial, antihuman immunodeficiency virus (HIV) and local anaesthetic agents.[23] 4*H*-Chromenes bearing amino and nitrile functionalities are also favoured medicinal compounds performing potential anticancer activity.[24,25] Moreover, a variety of functionalized 4*H*-chromene moieties appear as the key building block of numerous oxygen-containing natural products that exhibit diverse biological and pharmacological activities such as antiallergenic, antitumor, antineurodegenerative and anti-inflammatory effects.[26–29] Also, various chromene derivatives have found applications in different fields such as cosmetics, pigments and potentially biodegradable agrochemicals.[30] Conventional methods reported for the synthesis of chromenes generally employ a three-component reaction between malononitrile, 1,3-diketones and aldehydes. These reactions utilize different catalytic systems including hexadecyltrimethyl ammonium ionic liquids, Mg/La mixed metal oxides, nanosilica, bromide and silica-bonded propylpiperazine-*N*-sulfamic acid.[31]

In the present research, we describe for the first time the synthesis and characterization of Fe_3O_4-supported propane-1-sulfonic acid-grafted GO quantum dot (Fe_3O_4@GOQD-*O*-(propane-1-sulfonic acid)) and its application as an efficient and recyclable heterogeneous magnetic nanocatalyst for one-pot three-component synthesis of dihydropyrano[2,3-*c*]pyrazoles (**4a**–**4h**) and 4*H*-chromenes (**6a**–**6h**) (Scheme 1).

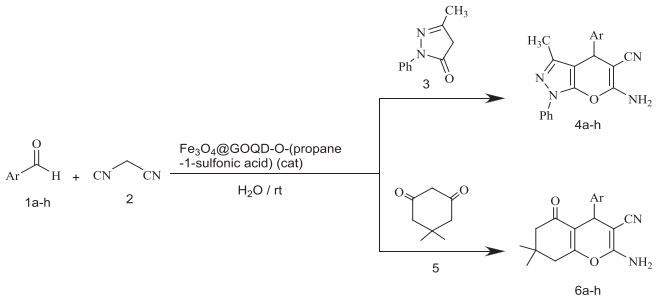

SCHEME 1 Synthesis of pyrano[2,3-*c*]pyrazoles **4a**–**4h** and 4*H*-chromenes **5a**–**5h** under the catalysis of Fe_3O_4@GOQD-*O*-(propane-1-sulfonic acid) nanocatalyst

2 | EXPERIMENTAL

2.1 | General

Chemicals including natural flake graphite (−325 mesh, 99.95%) were purchased from Merck chemical company and used as received. Melting points of organic compounds were measured in open capillary tubes with a Buchi 510 apparatus. Fourier transform infrared (FT-IR) spectra were recorded from KBr pellets using a Perkin Elmer Spectrum 65 FT-IR spectrophotometer. The progress of the reactions was monitored by TLC on Silica Gel PolyGram SIL G/UV 254 plates. NMR spectra were recorded for samples in $CDCl_3$ or DSMO-d_6 on 90 and 400 MHz BRUKER spectrometers using Me_4Si as internal standard. Energy-dispersive X-ray (EDX) analysis of the prepared catalyst was performed on a VG ESCALAB-200R spectrometer equipped with a hemispherical electron analyser. Magnetic property of the catalyst sample was measured with a vibrating sample magnetometer (VSM) model LBKFB, Meghnatis Daghigh Kavir Co, Iran, at room temperature. Qualitative analysis of Fe_3O_4@GOQD-*O*-(propane-1-sulfonic acid) magnetic nanosheets was performed on a scanning electron microscopy (SEM) and high-resolution transmission electron microscopy (HRTEM) images were obtained using a Zeiss model Zeiss-EM10C-100 KV field emission gun-scanning electron microscope (FESEM). Powder X-ray diffraction (XRD) was conducted on a PANalytical X'Pert PRO X-Ray Diffractometer.

2.2 | Preparation of GO

GO was synthesized following the modified Hummers' method as previously reported.[32] In the first step, 125 ml of H_2SO_4 was added to 2.5 g of graphite powder, and the mixture was stirred for 24 h. Next, to the resulting reaction mixture was slowly added 15 g of $KMnO_4$, and the reaction mixture was continuously stirred at 50°C for 72 h. Afterwards, the resulted mixture was poured into a beaker containing 250 ml of ice followed by addition of 25 ml of H_2O_2 (30%) in 250 ml of deionized (DI) water. As a result, the mixture was turned from brown colour into bright yellow. The resulted product was separated by centrifugation, washed with DI water and 10% HCl solution for three times and dried at 70°C.

2.3 | Synthesis of GOQDs

GO quantum dots (GOQDs) were synthesized using a simple process as previously reported.[33] GOQDs were prepared from the above-synthesized GO nanosheets. First, 0.6 g of GO was added to 120 ml of *N*,*N*-dimethylformamide (DMF) as a reducing agent and solvent, and the resulting mixture was heated at 250°C for 6 h. Afterwards, the precipitated reaction product was vacuum filtered using a 0.2-μm nylon membrane. Finally, the GOQDs as a black solid was obtained by evaporating the solvent under reduced pressure using a rotary evaporator and dried at 65°C.

2.4 | Preparation of Fe_3O_4-supported GO grafted with propane-1-sulfonic acid

2.4.1 | Acyl-chlorination of GOQDs

Initially, in a flask containing 60 ml of thionyl chloride was added GO (0.3 g) with stirring at 70°C under argon for 24 h. After completion of the reaction as monitored by TLC, the resulted acyl-chlorinated GOQDs product was centrifuged, washed with tetrahydrofuran (THF) four times and finally dried under vacuum.[12]

2.4.2 | Functionalization of GOQDs with 3-hydroxypropane-1-sulfonic acid

A total of 1 g of 3-hydroxypropane-1-sulfonic acid was added to the acyl-chlorinated GOQDs (0.3 g). Then, the mixture was refluxed for 72 h at 120°C under argon condition. The resulting solid material was washed with DI water to obtain the dark powder GOQD-*O*-(propane-1-sulfonic acid) product.[14]

2.4.3 | Nanomagnetization of GOQD-*O*-(propane-1-sulfonic acid)

Fe_3O_4@GOQD-*O*-(propane-1-sulfonic acid) was synthesized following a modified procedure reported by Kassaee et al.[34] The feeding weight ratio of m($FeCl_3$): m(GO) used in the prepared mixture was 20:1. Initially, 40 mg of previously prepared GOQD-*O*-(propane-1-sulfonic acid) in 40 ml of DI water was ultrasonicated for 30 min. Then, to the resulting mixture was added 50-ml solution of $FeCl_2$ (300 mg) and $FeCl_3$ (800 mg) in DI water (40 ml) at room temperature. Afterwards, the pH value of the mixture was increased to 11 by adding 30% aqueous solution of ammonia (30 ml), and the mixture was stirred at 75°C for 30 min. The final product was separated by using an external magnet,

washed with DI water for several times and dried at 65°C.

2.5 | General procedure for the synthesis of 1,4-dihydropyrano[2,3-*c*]pyrazole derivatives

To a mixture of aldehyde 1 (1 mmol), malononitrile (66 mg, 1 mmol) and 3-methyl-1-phenyl-1*H*-pyrazol-5(4*H*)-one (174 mg, 1 mmol) in DI water (5 ml) was added the catalyst Fe_3O_4@GOQD-*O*-(propane-1-sulfonic acid) (20 mg), and the mixture was stirred under room temperature for an appropriate time (Table 4). After completion of the reaction as monitored by TLC, the reaction mixture was diluted with hot ethanol (15 ml) and stirred for 5 min. Then, the catalyst was isolated by using an external magnet. The remaining supernatant liquid was evaporated under reduced pressure to leave the crude product which was purified by recrystallization from absolute EtOH. All the synthesized products **4a**–**4h** were known compounds and were characterized by their physical properties and spectral (FT-IR, ^{1}H NMR and ^{13}C NMR) analysis and compared with the reported corresponding data (Table 3). The characterization data for the selected products are available online in the supporting information section provided at the end of the article.

2.6 | General procedure for the synthesis of 4*H*-chromene derivatives

To a mixture of aromatic aldehyde 1 (1 mmol), malononitrile (66 mg, 1 mmol) and dimedone (14 mg, 1 mmol) in DI water (5 ml) was added Fe_3O_4@GOQD-*O*-(propane-1-sulfonic acid) (20 mg), and the resulting mixture was stirred at room temperature for an appropriate time (Table 5). After completion of the reaction as monitored by TLC, 15 ml of hot EtOH was added to the resulting reaction mixture and the catalyst was magnetically separated by using an external magnet. The solvent was removed under reduced pressure to leave the crude residue which was recrystallized from absolute EtOH to afford the pure product. The synthesized products **6a**–**6h** were all known compounds and were characterized based on their melting points and spectral (FT-IR, ^{1}H NMR and ^{13}C NMR) analysis and compared with the reported corresponding data (Table 4). The characterization data for the selected products are available online in the supporting information section provided at the end of the article.

3 | SELECTED DATA

3.1 | 6-Amino-3-methyl-1,4-diphenyl-1,4-dihydropyrano[2,3-*c*]pyrazole-5-carbonitrile (4a)

White solid; m.p. 170°C to 173°C; IR (KBr) (ν_{max}/cm^{-1}): 3471, 3324, 3194, 3063, 2917, 2198, 1659, 1593, 1516, 1385, 1265, 1066, 827, 753, 686, 651. ^{1}H NMR (90 MHz, $CDCl_3$) δ: 1.89 (s, 3*H*, CH_3), 4.66–4.69 (d, 3*H*, CH, NH_2), 7.28–7.61 (m, 10*H*, H—Ar) ppm. ^{13}C NMR (100 MHz, DMSO-d_6) δ: 13.0, 37.2, 58.7, 99.1, 116.5, 120.4, 126.6, 127.5, 128.2, 129.0, 129.8, 138.0, 144.0, 144.3, 145.7, 159.8 ppm.

3.2 | 6-Amino-4-(*p*-chlorophenyl)-3-methyl-1-phenyl-1,4-dihydropyrano[2,3-*c*]pyrazole-5-carbonitrile (4c)

White solid; m.p. 183°C to 186°C; IR (KBr) (ν_{max}/cm^{-1}): 3393, 3280, 3170, 2924, 2224, 2192, 1660, 1605, 1513, 1456, 1370, 1278, 1128, 1073, 936, 834, 759, 692, 669, 572. ^{1}H NMR (400 MHz, DMSO-d_6) δ: 1.80 (s, 3*H*, CH_3), 4.74 (s, 1*H*, CH), 7.28–7.81 (m, 11*H*, H—Ar and NH_2) ppm. ^{13}C NMR (100 MHz, DMSO-d_6) δ: 13.0, 36.5, 58.2, 98.7, 120.3, 120.4, 120.5, 126.7, 129.0, 129.6, 130.2, 132.1, 138.0, 143.1, 144.4, 145.7, 159.9 ppm.

3.3 | 6-Amino-4-(*p*-methoxyphenyl)-3-methyl-1-phenyl-1,4-dihydropyrano[2,3-*c*]pyrazole-5-carbonitrile (4e)

White solid; m.p. 170°C to 173°C; IR (KBr) (ν_{max}/cm^{-1}): 3390, 3321, 3204, 3022, 2191, 1660, 1583, 1513, 1391, 1259, 11,249, 1128, 1109, 1026, 839, 759, 692, 573. ^{1}H NMR (90 MHz, DMSO-d_6) δ: 1.78 (s, 3*H*, CH_3), 3.74 (s, 3*H*, CH_3), 4.62 (s, 1*H*, CH), 6.84–7.82 (m, 11*H*, H—Ar, NH_2) ppm. ^{13}C NMR (100 MHz, DMSO-d_6) δ: 12.4, 36.1, 54.6, 59.1, 98.3, 113.4, 119.8, 125.5, 128.4, 128.7, 135.0, 137.4, 143.6, 145.2, 158.0, 158.9 ppm.

3.4 | 6-Amino-4-(3-bromophenyl)-3-methyl-1-phenyl-1,4-dihydropyrano[2,3-*c*]pyrazole-5-carbonitrile (4h)

White solid; m.p. 161°C to 164°C; IR (KBr) (ν_{max}/cm^{-1}): 3450, 3324, 3195, 2199, 1660, 1593, 1518, 1487, 1456, 1391, 1126, 1065, 859, 751, 686. ^{1}H NMR (400 MHz, DMSO-d_6) δ: 1.81 (s, 3*H*, CH_3), 4.75 (s, 1*H*, CH), 7.29–7.35 (m, 5*H*, H—Ar), 7.47–7.52 (m, 4*H*, H—Ar), 7.79–7.81 (m, 2*H*, NH_2)

ppm. ^{13}C NMR (100 MHz, DMSO-d_6) δ: 13.1, 36.8, 58.0, 98.5, 120.4, 120.6, 122.3, 126.7, 127.5, 129.8, 130.5, 130.9, 131.3, 138.0, 144.4, 145.6, 146.9, 160.0 ppm.

3.5 | 6-Amino-3-methyl-4-(naphthalen-2-yl)-1-phenyl-1,4-dihydropyrano[2,3-*c*]pyrazole-5-carbonitrile (4i)

White solid; m.p. 192°C to 195°C; IR (KBr) (ν_{max}/cm^{-1}): 3471, 3327, 2195, 1662, 1595, 1519, 1366, 1126, 1069, 814, 749. ^{1}H NMR (400 MHz, DMSO-d_6) δ: 1.77 (s, 3*H*, CH_3), 4.88 (s, 1*H*, CH), 7.35–7.91 (m, 14*H*, H—Ar and NH_2) ppm. ^{13}C NMR (100 MHz, DMSO-d_6) δ: 13.5, 37.4, 58.5, 98.8, 120.4, 120.5, 126.3, 126.4, 126.6, 126.6, 126.7, 128.0, 128.2, 128.9, 129.8, 132.7, 133.3, 138.0, 141.3, 144.4, 145.8, 159.9, 159.9 ppm.

3.6 | 6-Amino-3-methyl-1-phenyl-4-(pyridin-3-yl)-1,4-dihydropyrano[2,3-*c*]pyrazole-5-carbonitrile (4j)

White solid; m.p. 227°C to 229°C; IR (KBr) (ν_{max}/cm^{-1}): 3365, 3299, 2191, 1659, 1588, 1519 cm^{-1}; ^{1}H NMR (400 MHz, DMSO-d_6) δ:1.86 (s, 3*H*, CH_3), 4.87 (s, 1*H*, C—H), 7.41–8.63 (m, 11*H*, H—Ar and NH_2) ppm; ^{13}C NMR (400 MHz, DMSO-d_6) δ: 12.5, 34.1, 57.1, 97.6, 119.8, 120.0, 123.8, 126.2, 129.0, 129.3, 135.5, 137.4, 138.9, 143.9, 145.0, 149.0, 149.1, 159.5, 159.6 ppm.

3.7 | 2-Amino-7,7-dimethyl-5-oxo-4-phenyl-5,6,7,8-tetrahydro-4*H*-chromene-3-carbonitrile (6a)

White solid; m.p. 235°C to 237°C; IR (KBr) (ν_{max}/cm^{-1}): 3394, 3324, 3251, 3212, 2960, 2889, 1680, 1604, 1413, 1371, 1249, 1214, 1159, 1138, 1071, 1036, 838, 695, 578. ^{1}H NMR (90 MHz, $CDCl_3$) δ: 1.04 (s, 3*H*, CH_3), 1.11 (s, 3*H*, CH_3), 2.23 (s, 2*H*, CH_2), 2.45 (s, 2*H*, CH_2), 4.41 (s, 1*H*, CH), 4.45 (s, 2*H*, NH_2), 7.24 (s, 5*H*, H—Ar) ppm; ^{13}C NMR (75.5 MHz, DMSO-d_6) δ: 26.8, 28.4, 31.8, 35.5, 49.9, 58.3, 112.7, 119.7, 127.1, 128.3, 144.7, 158.4, 162.5, 195.6 ppm.

3.8 | 2-Amino-7,7-dimethyl-4-(*p*-fluorphenyl)-5-oxo-5,6,7,8-tetrahydro-4*H*-chromene-3-carbonitrile (6b)

White solid; m.p. 188°C to 190°C; IR (KBr) (ν_{max}/cm^{-1}): 3354, 3178, 3100, 2960, 2190, 1674, 1636, 1603, 1504, 1410, 1366, 1261, 1215, 1160, 1139, 1033, 1015, 859, 561, 530, 487. ^{1}H NMR (300 MHz, DMSO-d_6) δ: 0.93 (s, 3*H*, CH_3), 1.02 (s, 3*H*, CH_3), 2.05–2.27 (m, 2*H*, CH_2), 2.50 (s, 2*H*, CH_2), 4.15 (s, 1*H*, CH), 6.98–7.27 (m, 6*H*, H—Ar and NH_2) ppm; ^{13}C NMR (100 MHz, DMSO-d_6) δ: 27.2, 28.8, 32.2, 35.9, 38.9, 50.4, 58.8, 113.1, 120.2, 127.1, 127.6, 128.8, 145.1, 158.9, 163.1, 196.4 ppm.

3.9 | 2-Amino-4-(*p*-cholorphenyl)-7,7-dimethyl-5-oxo-5,6,7,8-tetrahydro-4*H*-chromene-3-carbonitrile (6d)

White solid; m.p. 211°C to 214°C; IR (KBr) (ν_{max}/cm^{-1}): 3379, 3323, 3180, 2958, 2942, 2887, 2188, 1675, 1634, 1390, 1286, 1215, 1093, 1014, 884, 854, 769, 639, 620, 576. ^{1}H NMR (90 MHz, DMSO-d_6) δ: 0.94 (s, 3*H*, CH_3), 1.03 (s, 3*H*, CH_3), 2.15 (s, 2*H*, CH_2), 2.50 (s, 2*H*, CH_2), 4.195 (s, 1*H*, CH), 7.05–7.30 (s, 6*H*, H—Ar and NH_2) ppm; ^{13}C NMR (100 MHz, DMSO-d_6) δ:14.0, 20.7, 26.8, 28.3, 31.8, 35.1, 49.9, 57.7, 59.7, 112.3, 119.5, 128.2, 129.1, 131.1, 143.7, 158.5, 162.6, 170.3 ppm.

3.10 | 2-Amino-7,7-dimethyl-4-(*p*-nitrophenyl)-5-oxo-5,6,7,8-tetrahydro-4*H*-chromene-3-carbonitrile (6g)

Cream solid; m.p. 178°C to 181°C; IR (KBr) (ν_{max}/cm^{-1}): 3406, 3316, 3176, 2977, 2942, 2183, 1672, 1631, 1521, 1493, 1390, 1296, 1159, 1031, 855, 729, 629, 617, 574, 561. ^{1}H NMR (90 MHz, DMSO-d_6) δ: 0.96 (s, 3*H*, CH_3), 1.04 (s, 3*H*, CH_3), 2.17 (s, 2*H*, CH_2), 2.53 (s, 2*H*, CH_2), 4.37 (s, 1*H*, CH), 7.18–7.18 (m, 4*H*, H—Ar), 8.12 (s, 2*H*, NH_2) ppm. ^{13}C NMR (100 MHz, DMSO-d_6) δ: 26.9, 28.2, 31.8, 35.6, 39.6, 49.8, 56.9, 111.7, 119.3, 123.7, 128.6, 146.2, 152.3, 158.5, 163.1, 195.7 ppm.

3.11 | 2-Amino-4-(*m*-chlorophenyl)-7,7-dimethyl-5-oxo-5,6,7,8-tetrahydro-4*H*-chromene-3-carbonitrile (6i)

White solid, m.p. 222°C to 225°C, IR (KBr) (ν_{max}/cm^{-1}): 3394, 3329, 3198, 2960, 2199, 1682, 1654, 1604, 1370, 1214. ^{1}H NMR (90 MHz, DMSO-d_6) δ: 0.94 (s, 3*H*, CH_3), 1.01 (s, 3*H*, CH_3), 2.07–2.27 (m, 2*H*, CH_2), 2.51 (s, 2*H*, CH_2), 4.198 (s, 1*H*, CH), 7.091–7.34 (m, 6*H*, H—Ar, NH_2) ppm. ^{13}C NMR (100 MHz DMSO-d_6) δ: 27.2, 28.7, 32.2, 35.7, 50.3, 58.0, 112.4, 120.0, 126.3, 127.1, 127.4, 130.7, 133.3, 147.6, 158.9, 113.4, 196.3 ppm.

3.12 | 2-Amino-7,7-dimethyl-5-oxo-4-(thiophen-2-yl)-5,6,7,8-tetrahydro-4*H*-chromene-3-carbonitrile (6j)

White solid, m.p. 200°C to 202°C, IR (KBr) (ν_{max}/cm^{-1}): 3382, 3321, 3208, 2963, 2878, 2198, 1678, 1660, 1602, 1466, 1374, 1214. ^{1}H NMR (400 MHz, DMSO-d_6) δ: 0.98 (s, 3*H*, CH_3), 1.05 (s, 3*H*, CH_3), 2.1–2.2 (s, 2*H*, CH_2), 2.4–2.5 (s, 2*H*, CH_2), 4.5 (s, 1*H*, CH), 6.6–6.9 (m, 2*H*, H—Ar), 7.1–7.3 (s, H, H—CS, s, 2*H*, NH_2) ppm. ^{13}C NMR (400 MHz DMSO-d_6) δ: 26.4, 28.6, 30.3, 31.7, 49.8, 57.9, 112.8, 119.5, 123.9, 124.3, 126.7, 149.2, 158.8, 162.4, 195.5 ppm.

4 | RESULTS AND DISCUSSION

4.1 | Characterization of the catalyst Fe_3O_4@GOQD-*O*-(propane-1-sulfonic acid)

The Fe_3O_4@GOQD-*O*-(propane-1-sulfonic acid) magnetic nanosheets were prepared by a simple five-step procedure presented in Scheme 2. As shown in this scheme, GO was initially prepared according to the Hummers' method.[32] Then, GOQDs was synthesized by a simple process from freshly prepared GO via treatment with *N*,*N*-DMF at 250°C for 6 h.[33] In the next step, the GOQD-*O*-(propane-1-sulfonic acid) nanosheets were obtained by acyl-chlorination of GOQDs followed by modification with 3-hydroxypropane-1-sulfonic acid. Finally, the Fe_3O_4@GOQD-*O*-(propane-1-sulfonic acid) magnetic nanosheets were obtained by coprecipitation of ferrous (Fe^{2+}) and ferric (Fe^{3+}) ions in the presence of the prepared GOQD-*O*-(propane-1-sulfonic acid) according to the method reported by Kassaee et al.[34]

The structure of the synthesized magnetic nanosheets was fully characterized by different analytical techniques as described below.

Figure 1 illustrates the FT-IR spectra of the GO, GOQDs, and Fe_3O_4@GOQD-*O*-(propane-1-sulfonic acid) magnetic nanosheets. The peaks at 1717, 1627 and 1107 cm^{-1} shown in the spectra of GO and GOQDs are assigned to the stretching vibrations of C═O, C═C and C—O groups, respectively.[44] The O—H stretching vibration due to the hydroxy, carboxylic and enolic groups of the GO is observed in the range 2760–3440 cm^{-1} for all three compounds. Also, the peak shown at 1388 cm^{-1} in the spectra of the GO and GOQDs can be attributed to the asymmetric stretching vibration of the C—O—C moiety in the epoxide groups which has appeared in Figures 1a and 2b. Similarity shown between the infrared spectra of GO (Figure 1a) and GOQDs (Figure 1b) illustrates that the structure of GO has remained intact in the presence of DMF during the synthesis of GOQD. This result combined with the TEM analysis clearly confirmed the successful synthesis of GOQD in the presence of DMF.[33]

The absorption band at 1022 cm^{-1} in the spectrum of the magnetized 1-propane sulfonic acid-grafted GOQDs Fe_3O_4@GOQD-*O*-(propane-1-sulfonic acid) (Figure 1c) corresponds to the vibrational frequency of ν(S═O) related to the SO_3H group. Also, the presence of SO_3 group was confirmed by the peak at 1221 cm^{-1}.[10,45] In addition, the peaks at 2920 and 2850 cm^{-1} in Figure 1c are assigned to C—H stretching vibrations of the propyl group attached to the sulfonic acid group. In the spectrum of Fe_3O_4@GOQD-*O*-(propane-1-sulfonic acid), the absorption bands observed at around 620 and 485 cm^{-1} are related to the Fe—O stretching vibrations.[46,47] As seen in the spectrum of the magnetized sulfonated GOQDs, the stretching frequency of the carboxyl and ester groups has been shifted from 1730 cm^{-1} to a lower frequency at 1618 cm^{-1} that could be explained by the change of COOH groups to carboxylate (COO^-) groups upon magnetization with Fe_3O_4.[48] These results indicated that the GOQD was successfully modified with propane-1-sulfonic acid group as supported by the spectrum of the magnetic Fe_3O_4 NPs.

The XRD patterns obtained from the GO and the prepared Fe_3O_4@GOQD-*O*-(propane-1-sulfonic acid) are illustrated in Figure 2a,b. According to Figure 2a, GO exhibits main diffraction peaks at $2\theta = 11.95°$ and 42.45° corresponding to the indices (002) and (100), respectively.[49] The peak at $2\theta = 11.8°$ exhibited by GO has been significantly shifted at about $2\theta = 24°$ as a result of magnetization with Fe_3O_4. The relative intensities and positions of all the peaks shown at $2\theta = 30.39°$, 35.74°, 43.36°, 57.31° and 62.93° in the XRD pattern of Fe_3O_4@GOQD-*O*-(propane-1-sulfonic acid) are in compliance with standard XRD pattern of magnetite Fe_3O_4 (JCPDS Card No. 79-0417).[50] These results indicated that the GOQDs films were successfully magnetized with Fe_3O_4 and grafted with propane-1-sulfonic acid group.[48–51]

The elemental composition of the Fe_3O_4@GOQD-*O*-(propane-1-sulfonic acid) was established by EDX analysis. The EDX images obtained from the samples (Figure 3) clearly indicated the expected components (C, O, S and Fe) of the Fe_3O_4@GOQD-*O*-(propane-1-sulfonic acid). The atomic weight ratios of the corresponding elements calculated from the EDX analysis are listed in Table 1. These results provided further evidence for successful grafting of GOQDs films with propane-1-sulfonic acid group and magnetization with Fe_3O_4 MNPs.

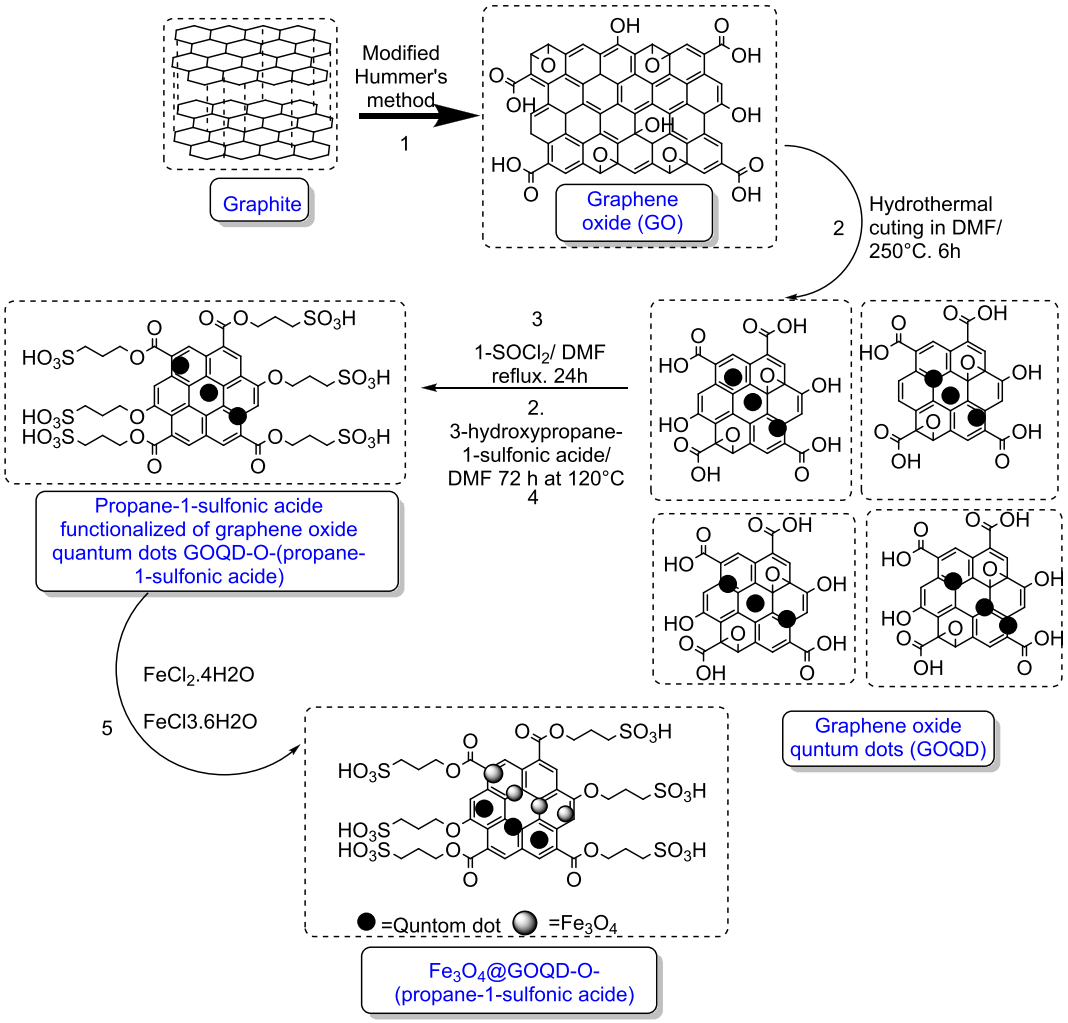

SCHEME 2 Synthetic route to nanomagnetic Fe_3O_4-supported 1-propane sulfonic acid-grafted graphene oxide quantum dots Fe_3O_4@GOQDs-*O*-(propane-1-sulfonic acid)

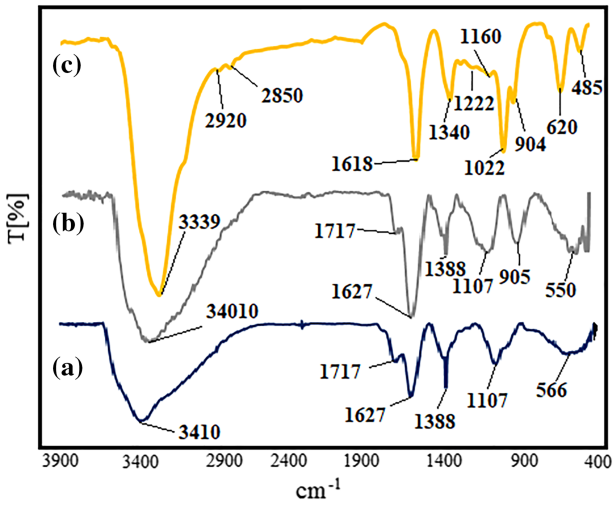

FIGURE 1 Comparative Fourier transform infrared (FT-IR) spectra for (a) graphene oxide (GO), (b) graphene oxide quantum dots (GOQDs) and (c) Fe_3O_4@GOQD-*O*-(propane-1-sulfonic acid)

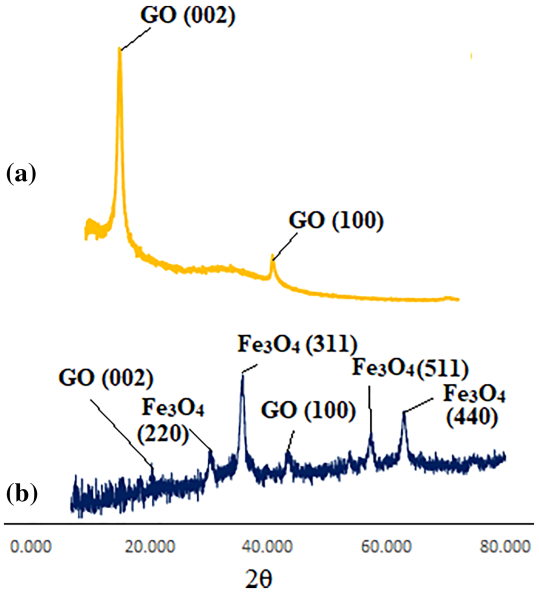

FIGURE 2 X-ray diffraction (XRD) patterns of (a) graphene oxide (GO) and (b) Fe_3O_4@GOQD-*O*-(propane-1-sulfonic acid)

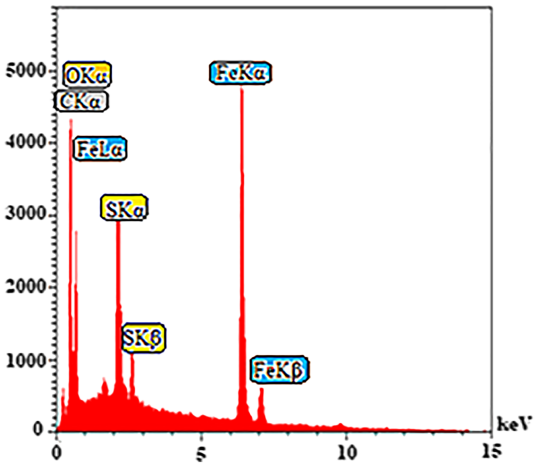

FIGURE 3 The energy-dispersive X-ray (EDX) images of Fe_3O_4@GOQD-*O*-(propane-1-sulfonic acid)

TABLE 1 Elemental quantitative analysis of Fe_3O_4@GOQD-*O*-(propane-1-sulfonic acid) derived from energy-dispersive X-ray (EDX)

Fe_3O_4@GOQD-*O*-(propane-1-sulfonic acid)		
Element	**Weight%**	**Atomic%**
C	6.86	14.41
O	33.39	52.79
S	17.21	13.59
Fe	42.54	19.21
Total	100.00	100.00

Thermal stability of the Fe_3O_4@GOQD-*O*-(propane-1-sulfonic acid) nanosheets was studied by thermal gravimetric analysis (TGA). According to the TGA thermogram shown in Figure 4, the first weight loss (~4.34) of the Fe_3O_4@GOQD-*O*-(propane-1-sulfonic acid) takes place below 120°C due to the thermal desorption of the adsorbed water and remaining organic solvent. The second weight loss of about 8% occurring at around 212°C is attributed to the decomposition of the oxygen-containing groups on the surface of GOQDs. The third and fourth total weight loss happening in the range 240°C to 600°C is due to the complete removal of the organic and inorganic segments from the surface of GOQD.[34,52,53] These results clearly provide further evidence for successful functionalization of GOQDs by 1-propane sulfonic acid group and its magnetization with Fe_3O_4 NP as well.

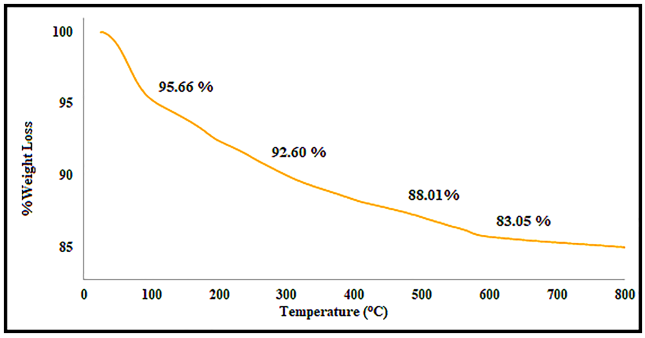

FIGURE 4 Thermal gravimetric analysis (TGA) curves of Fe_3O_4@GOQD-*O*-(propane-1-sulfonic acid)

The scanning electron microscope (FESEM) analysis was performed on the prepared nanosheets of GO, GOQDs and Fe_3O_4@GOQD-*O*-(propane-1-sulfonic acid) in order to find their morphology and size distribution. As revealed from the comparison between the FESEM patterns of the naked GO and GOQD, no prominent change on the morphology of GO films has occurred as a result of cutting by DMF. Transition electron microscopic (TEM) analysis was conducted on the GOQDs nanosheets in order to study the structure of the GOQDs clusters. The TEM images obtained from GOQDs (Figure 5c) indicates the number of GOQDs clusters as well as its size distribution. The SEM images displayed in Figure 5 indicated that the Fe_3O_4@GOQD-*O*-(propane-1-sulfonic acid) nanocomposite is composed of wrinkled thin films closely associated with each other to form disordered solids and randomly accumulated. Moreover, the FESEM image of the Fe_3O_4@GOQD-SO Fe_3O_4@GOQD-*O*-(propane-1-sulfonic acid) catalyst (Figure 5c) indicated that the Fe_3O_4 NPs exhibited a regularly spherical morphology on Fe_3O_4@GOQD-*O*-(propane-1-sulfonic acid) which are made up of nanosized films.[45]

The morphology and size distribution of the prepared GOQDs was investigated using TEM images. As shown in Figure 6, the numbers of quantum dots, size distribution and clusters of the GOQDs were clearly shown, and the average diameter was estimated to be in the range 5–11 nm. The results obtained from TEM image of the GOQDs nanosheets indicated that the GO has been successfully converted to the GOQDs.[54]

In addition to the above-mentioned FT-IR, TGA, XRD, EDX, SEM and TEM analyses, the magnetization behaviour of the prepared Fe_3O_4@GOQD-*O*-(propane-1-sulfonic acid) was examined by VSM analysis at 300 K. According to the typical curves of magnetization versus the applied magnetic field of Fe_3O_4@GOQD-*O*-(propane-1-sulfonic acid) shown in Figure 7, the saturation magnetization (M_s) value of Fe_3O_4@GOQD-*O*-(propane-1-sulfonic acid) was found to be 49 emu g^{-1}. This saturation magnetization value approved the superparamagnetic property of the Fe_3O_4@GOQD-*O*-(propane-1-sulfonic acid) nanocatalyst which enables it to be efficiently separated from the reaction mixture simply by using an external magnet.

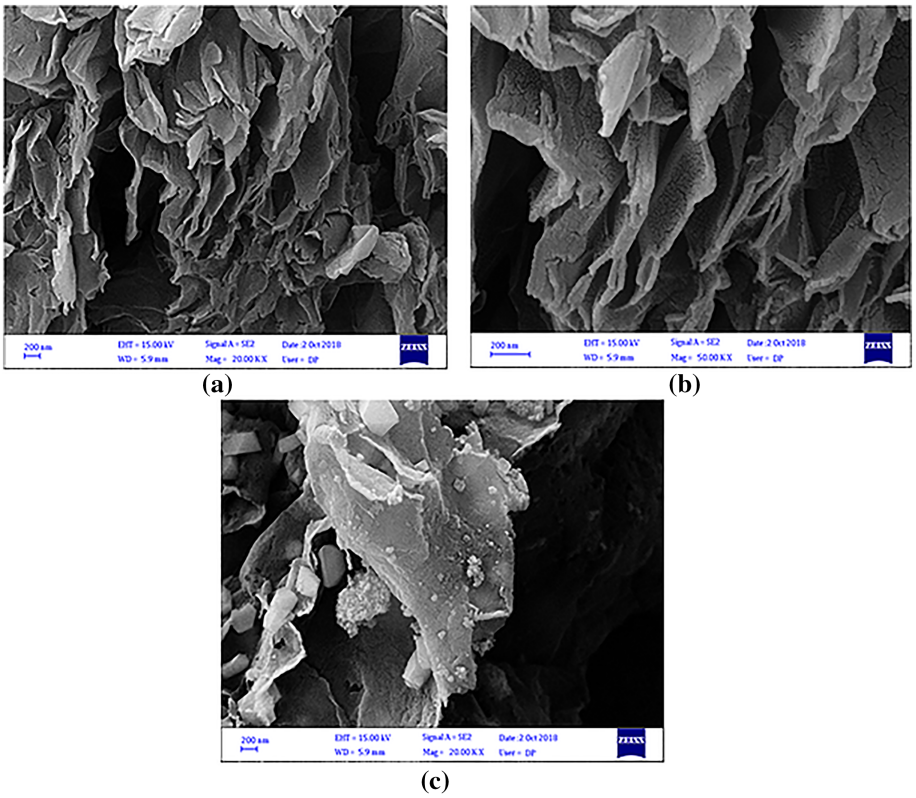

FIGURE 5 Field emission gun-scanning electron microscope (FESEM) images of (a) graphene oxide (GO), (b) graphene oxide quantum dots (GOQDs) and (c) Fe_3O_4@GOQD-*O*-(propane-1-sulfonic acid)

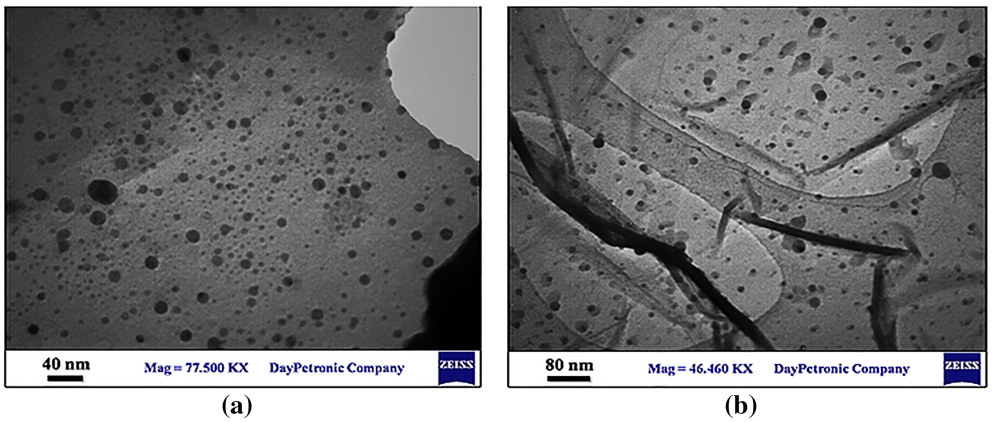

FIGURE 6 Transition electron microscopic (TEM) images of graphene oxide quantum dots (GOQDs)

4.2 | Catalytic activity

The catalytic capability of the synthesized Fe_3O_4@GOQD-*O*-(propane-1-sulfonic acid) magnetic nanosheets was examined in one-pot synthesis of dihydropyrano[2,3-*c*]pyrazole and 4*H*-chromene derivatives. The procedure involves three-component reactions between aromatic aldehyde, malononitrile and 3-methyl-1-phenyl-1*H*-pyrazol-5(4*H*)-one or dimedone as shown in Scheme 3. *p*-Nitrobenzaldehyde was chosen as the test aromatic compound in this reaction to optimize different reaction parameters such as solvent, temperature and catalyst loading. According to the results summarized in Table 2, the best result in terms of the reaction rate and yield of the product dihydropyrano[2,3-*c*]pyrazole was obtained when the reaction was carried out in H_2O as the solvent at room temperature using 10-mg catalyst loading (Entry 2).

Similarly, in order to find the optimal conditions for the possible formation of 4*H*-chromene derivatives, we chose to study one-pot three-component reaction between 4-nitrobenzaldehyde, malononitrile and 5,5-dimethyl-1,3-cyclohexanedione (dimedone) as model reaction (Scheme 4). The effects of different reaction parameters including the solvent, temperature and catalyst loading on this reaction were studied. According to the experimental results summarized in Table 3, the best result in terms of the reaction rate and yield of the

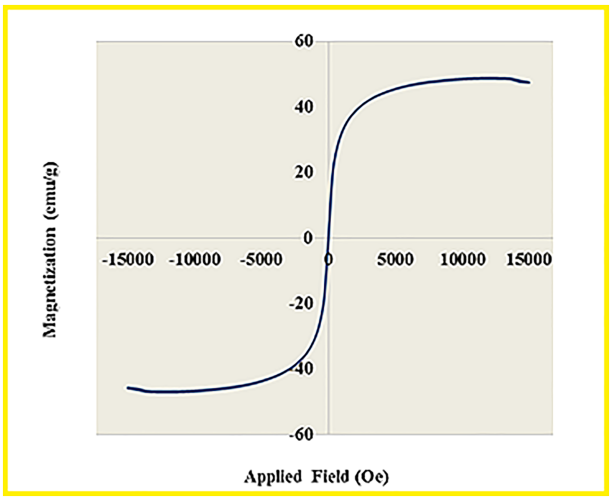

FIGURE 7 Vibrating sample magnetometer (VSM) image of Fe_3O_4@GOQD-*O*-(propane-1-sulfonic acid)

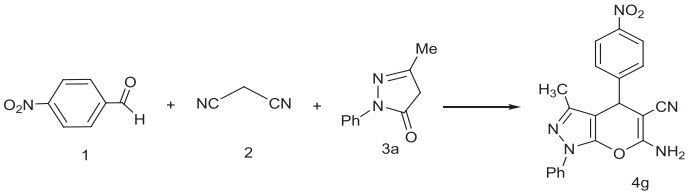

SCHEME 3 Screening the reaction parameters for the model synthesis of 6-amino-3-methyl-4-(*p*-nitrophenyl)-1-phenyl-1,4-dihydropyrano[2,3-*c*]pyrazole-5-carbonitrile

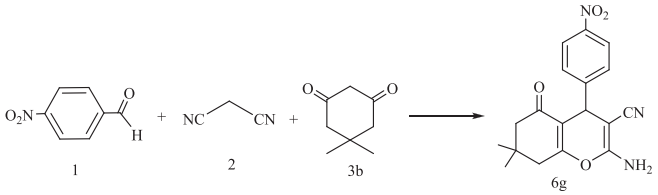

SCHEME 4 Screening the reaction parameters for model synthesis of 2-amino-4-(*p*-nitrophenyl)-7,7-dimethyl-5-oxo-5,6,7,8-tetrahydro-4*H*-chromene-3-carbonitrile

product was obtained when the reaction was carried out in H_2O at room temperature in the presence of 10 mg of the catalyst (Entry 2). Indispensable use of the catalyst Fe_3O_4@GOQD-*O*-(propane-1-sulfonic acid) in the reaction was verified by carrying out the reaction under the optimal conditions without using the catalyst and noticed that no detectable amount of the respected product was formed (Entry 14).

Following the remarkable effect of Fe_3O_4@GOQD-*O*-(propane-1-sulfonic acid) as an efficient nanocatalyst in the model reaction, the generality and scope of the reaction was established by using a diverse series of aromatic aldehydes **1a**–**1h** in the reaction under optimal conditions (Schemes 5 and 6). The experimental results summarized in Tables 4 and 5 demonstrated that all the reactions proceeded smoothly to afford the products in excellent yields (90–98%) irrespective of the nature of the

TABLE 2 Screening the reaction parameters for the model synthesis of 6-amino-3-methyl-4-(*p*-nitrophenyl)-1-phenyl-1,4-dihydropyrano[2,3-*c*]pyrazole-5-carbonitrile (Scheme 3)

Entry	Catalyst loading (mg)	Solvent	Temperature (°C)	Time (min)	Yield[a] (%)
1	10	No solvent	25	280	trace
2	10	H_2O	25	45	98
3	10	EtOH	25	120	50
4	10	THF	25	180	30
5	10	DMF	25	220	42
6	10	H_2O	50	40	75
7	10	H_2O	80	35	85
8	10	H_2O	100	30	85
9	10	H_2O	rt	10	98
10	5	H_2O	rt	55	80
11	20	H_2O	rt	60	70
12	30	H_2O	rt	80	78
13	40	H_2O	rt	80	82
14	No catalyst	H_2O	rt	240	trace

Note: Conditions: 4-nitrobenzaldehyde (1.1 mmol), 4-hydroxyquinolin-2(1*H*)-one (1 mmol), malononitrile (1.1 mmol), solvent (5 ml).
[a]Isolated yields.

TABLE 3 Screening the reaction parameters for model synthesis of 2-amino-4-(*p*-nitrophenyl)-7,7-dimethyl-5-oxo-5,6,7,8-tetrahydro-4*H*-chromene-3-carbonitrile (Scheme 4)

Entry	Catalyst loading (mg)	Solvent	Temperature (°C)	Time (min)	Yield[a] (%)
1	10	No solvent	25	240	10
2	10	H_2O	25	15	97
3	10	EtOH	25	100	45
4	10	THF	25	280	25
5	10	DMF	25	120	35
6	10	H_2O	50	55	72
7	10	H_2O	80	50	85
8	10	H_2O	100	40	87
9	10	H_2O	rt	15	97
10	5	H_2O	rt	50	79
11	20	H_2O	rt	40	81
12	30	H_2O	rt	40	82
13	40	H_2O	Reflux	30	87
14	No catalyst	H_2O	Reflux	320	Trace

Note: Conditions: 4-nitrobenzaldehyde (1.1 mmol), 4-hydroxyquinolin-2(1*H*)-one (1 mmol), malononitrile (1.1 mmol), solvent (5 ml).
[a]Isolated yields.

SCHEME 5 Synthesis of 1,4-dihydropyrano[2,3-*c*] pyrazole derivatives catalysed by Fe_3O_4@GOQD-*O*-(propane-1-sulfonic acid)

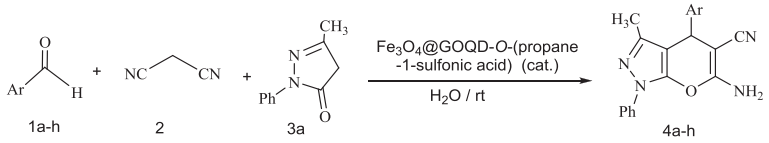

SCHEME 6 Synthesis of 2-amino-4-aryl-7,7-dimethyl-5-oxo-5,6,7,8-tetrahydro-4*H*-chromene-3-carbonitrile derivatives catalysed by Fe_3O_4@GOQD-*O*-(propane-1-sulfonic acid)

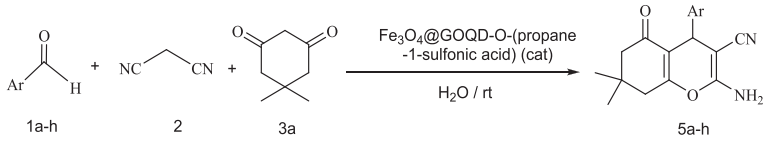

substituting groups attached to the aldehydes. However, the aromatic aldehydes carrying electron-withdrawing groups appear to act more readily in this reaction.

According to the experimental results summarized in Tables 6 and 7, the *magnetic nanocomposite film* (Fe_3O_4@GOQD-*O*-(propane-1-sulfonic acid)) exhibited high *catalytic activity* in comparison with the *catalytic activities* of the bare Fe_3O_4, GO and GOQDs under the same optimal conditions. The high EcoScale score of the present protocol compared with different other catalysts calculated from the reported method demonstrated that the present catalyst is greener in comparison with other catalysts examined in Tables 6 and 7.[55] All the fragments present in the catalyst perform a synergistic effect on the synthesis of dihydropyrano[2,3-*c*]pyrazole and 4*H*-chromene derivatives. According to the Tables 6 and 7, every part of the catalyst including GO, GOQD and Fe_3O_4 NP has individually low improvement effect on the reaction. However, when these parts are jointly present in the Fe_3O_4@GOQD-*O*-(propane-1-sulfonic acid) nanocomposite film can display high promotional effect in the synthesis of the titled reaction products (Schemes 7 and 8).

As summarized in Table 8, the experimental data resulted from the present protocol are compared with those reported by other research groups for the synthesis of 1,4-dihydropyrano[2,3-*c*]pyrazoles and 4*H*-chromenes employing different catalytic systems. From this comparison, it became evident that the present protocol is more eco-friendly and straightforward and the newly presented Fe_3O_4@GOQD-*O*-(propane-1-sulfonic acid) nanocomposite film performs high catalytic activity in the titled reactions. Therefore, the present method could be considered as a suitable alternative method for the synthesis of 1,4-dihydropyrano[2,3-*c*]pyrazoles and 4*H*-chromene derivatives.

TABLE 4 Synthesis of 1,4-dihydropyrano[2,3-*c*]pyrazole derivatives catalysed by Fe_3O_4@GOQD-*O*-(propane-1-sulfonic acid) (Scheme 5)

Entry	Ar	Product	Time (min)	Yield[a] (%)	m.p. (°C)	
					Found	Reported
1	C_6H_5	**4a**	25	93	163–166	161–163 (Guo et al.[35])
2	2-ClC_6H_4	**4b**	30	95	145–148	145–146 (Guo et al.[35])
3	4-ClC_6H_4	**4c**	30	96	183–186	184–187 (Sharanina et al.[36])
4	4-FC_6H_4	**4d**	20	97	173–176	174–177 (Sharanina et al.[36])
5	4-$MeOC_6H_4$	**4e**	45	95	170–173	171–172 (Sharanina et al.[36])
6	3-$NO_2C_6H_4$	**4f**	30	90	190–193	190–191 (Sharanina et al.[36])
7	4-$NO_2C_6H_4$	**4g**	10	98	186–189	186–188 (Saha et al.[37])
8	3-BrC_6H_4	**4h**	45	96	161–164	160–163 (Farahi et al.[38])
9	Naphthalen-2-yl	**4i**	30	95	192–195	-
10	Pyridin-3-yl	**4j**	40	94	226–229	227–229 (Vasuki et al.[22])
11	Thiopen-2-yl	**4k**	180	Trace	-	-
12	Furan-2-yl	**4l**	180	Trace	-	-
13	*n*-C_3H_7	**4m**	180	Trace	-	-

Note: Conditions: aldehyde (1.1 mmol), 3-methyl-1-phenyl-2-pyrazolin-5-one (1 mmol), malononitrile (1.1 mmol), H_2O (5 ml), catalyst (10 mg), room temperature.
[a]Isolated yields.

TABLE 5 Synthesis of 2-amino-4-aryl-7,7-dimethyl-5-oxo-5,6,7,8-tetrahydro-4*H*-chromene-3-carbonitrile derivatives catalysed by Fe_3O_4@GOQD-*O*-(propane-1-sulfonic acid) (Scheme 6)

Entry	Ar	Product	Time (min)	Yield[a] (%)	m.p. (°C)	
					Found	Reported
1	C_6H_5	**6a**	35	93	232–235	231–233 (Azarifar et al.[39])
2	4-FC_6H_4	**6b**	30	95	188–190	189–191 (Fang et al.[40])
3	4-MeC_6H_4	**6c**	40	93	207–210	211–213 (Azarifar et al.[39])
4	4-ClC_6H_4	**6d**	20	94	211–214	212–214 (Khaksar et al.[41])
5	2-ClC_6H_4	**6e**	40	96	211–214	212–214 (Khaksar et al.[41])
6	3-$NO_2C_6H_4$	**6f**	45	92	209–212	210–211 (Balalaie et al.[42])
7	4-$NO_2C_6H_4$	**6g**	15	97	178–181	178–180 (Balalaie et al.[42])
8	4-HOC_6H_4	**6h**	45	91	203–206	204–205 (Sarrafi et al.[43])
9	3-ClC_6H_4	**6i**	15	95	222–225	222–224 (Azarifar and Abbasi[21])
10	Thiopen-2-yl	**6j**	25	93	201–204	200–202 (Vasuki et al.[22])
11	Furan-2-yl	**6k**	180	Trace	-	-
12	*n*-C_3H_7	**6l**	180	Trace	-	-

Note: Conditions: aldehyde (1.1 mmol), dimedone (1 mmol), malononitrile (1.1 mmol), H_2O (5 ml), catalyst (10 mg), room temperature.
[a]Isolated yields.

TABLE 6 Comparative catalytic activity of Fe_3O_4@GOQD-*O*-(propane-1-sulfonic acid) nanoparticles under optimal conditions for synthesis of 6-amino-3-methyl-4-(4-nitrophenyl)-1-phenyl-1,4-dihydropyrano[2,3-*c*]pyrazole-5-carbonitrile based on EcoScale percentages and other reaction parameters

Entry	Catalyst	Time (min)	Yield (%)	Catalyst loading (g)	EcoScale (%)
1	GO	120	61	0.1	80
2	GOQDs	80	65	0.1	82
3	Fe_3O_4	60	68	0.1	70
4	Fe_3O_4@GOQD-*O*-(propane-1-sulfonic acid)	10	98	0.1	90

TABLE 7 Comparative catalytic activity of Fe_3O_4@GOQD-*O*-(propane-1-sulfonic acid) nanoparticles under optimal conditions for synthesis of 2-amino-7,7-dimethyl-4-(4-nitrophenyl)-5-oxo-5,6,7,8-tetrahydro-4*H*-chromene-3-carbonitrile based on EcoScale percentages and other reaction parameters

Entry	Catalyst	Time (min)	Yield (%)	Catalyst loading (g)	EcoScale (%)
1	GO	180	55	0.1	81
2	GOQDs	120	65	0.1	83
3	Fe_3O_4	100	70	0.1	74
5	Fe_3O_4@GOQD-*O*-(propane-1-sulfonic acid)	15	97	0.1	91

SCHEME 7 Comparative catalytic activity of Fe_3O_4@GOQD-*O*-(propane-1-sulfonic acid) nanoparticles under optimal conditions for synthesis of 6-amino-3-methyl-4-(4-nitrophenyl)-1-phenyl-1,4-dihydropyrano[2,3-*c*]pyrazole-5-carbonitrile

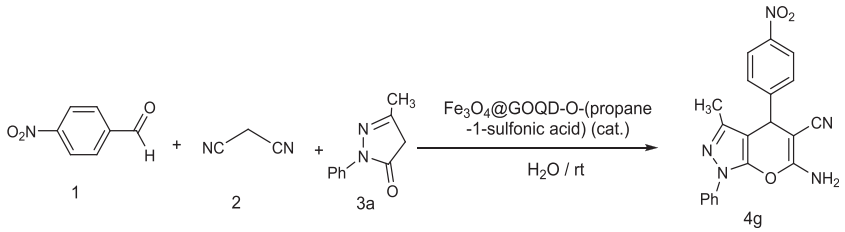

SCHEME 8 Comparative catalytic activity of Fe_3O_4@GOQD-*O*-(propane-1-sulfonic acid) nanoparticles under optimal conditions for synthesis of 2-amino-7,7-dimethyl-4-(4-nitrophenyl)-5-oxo-5,6,7,8-tetrahydro-4*H*-chromene-3-carbonitrile

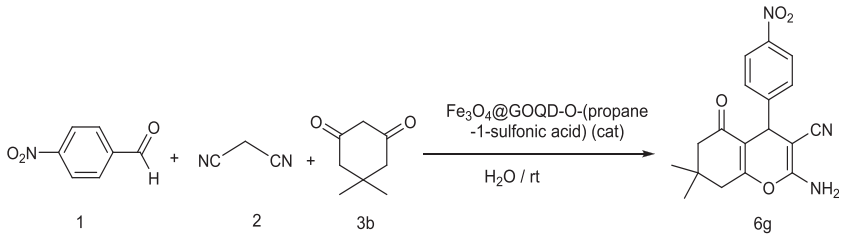

TABLE 8 Comparison of the present method with other methods reported for the synthesis of 1,4-dihydropyrano[2,3-*c*]pyrazole (product **4g**) and 2-amino-4-aryl-7,7-dimethyl-5-oxo-5,6,7,8-tetrahydro-4*H*-chromene-3-carbonitrile (product **6g**) derivatives

Entry	Catalyst	Conditions	Time (min)	Yield (%)	Product	Reference
1	BF_3/MNPs-450	EtOH; reflux	10	90	**4g**	Abdollahi-Alibeik et al.[56]
2	BS-2G-Ti	H_2O; 70°C	90	96	**4g**	Sinija and Sreekumar[57]
3	Silica-bonded *N*-propyl piperazine	EtOH; reflux	15	88	**4g**	Niknam et al.[58]
4	$NH_4H_2PO_4/Al_2O_3$	Glycerol; rt	12	73	**4g**	Abdel Hamid et al.[59]
5	Fe_3O_4@GOQD-*O*-(propane-1-sulfonic acid)	H_2O; rt	10	98	**4g**	Present work
6	Pectin	H_2O: EtOH; rt	20	90	**6g**	Kangani et al.[60]
7	[DABCO-PDO] [CH_3COO]	H_2O; 60°C	10	96	**6g**	Yang et al.[61]
8	$NH_4Al(SO_4)_2{\cdot}12H_2O$	EtOH; 80°C	140	85	**6g**	Mohammadi et al.[62]
9	Fructose	EtOH: H_2O; 60°C	10	89	**6g**	Pourpanah et al.[63]
10	Fe_3O_4@GOQD-*O*-(propane-1-sulfonic acid)	H_2O; rt	10	97	**6g**	Present work

4.3 | Catalytic reaction mechanism

The presence of various functionalities including carbonyl, hydroxyl and epoxy groups on the surface of the GO as basic and acidic groups, as well as the attached β-alanine moiety containing both amino and acidic groups, collectively make the catalyst Fe_3O_4@GOQD-*O*-(propane-1-sulfonic acid) more efficient in the reaction.

Also, the magnetic property generated by the Fe_3O_4 unit in the catalyst can promote the catalytic efficiency and enables easy magnetic separation of the catalyst from the reaction mixture.

A plausible mechanism proposed to explain the Fe_3O_4@GOQD-*O*-(propane-1-sulfonic acid)-catalysed one-pot synthesis of 1,4-dihydropyrano[2,3-*c*]pyrazoles is depicted in Scheme 7. Likely, in the first step, the

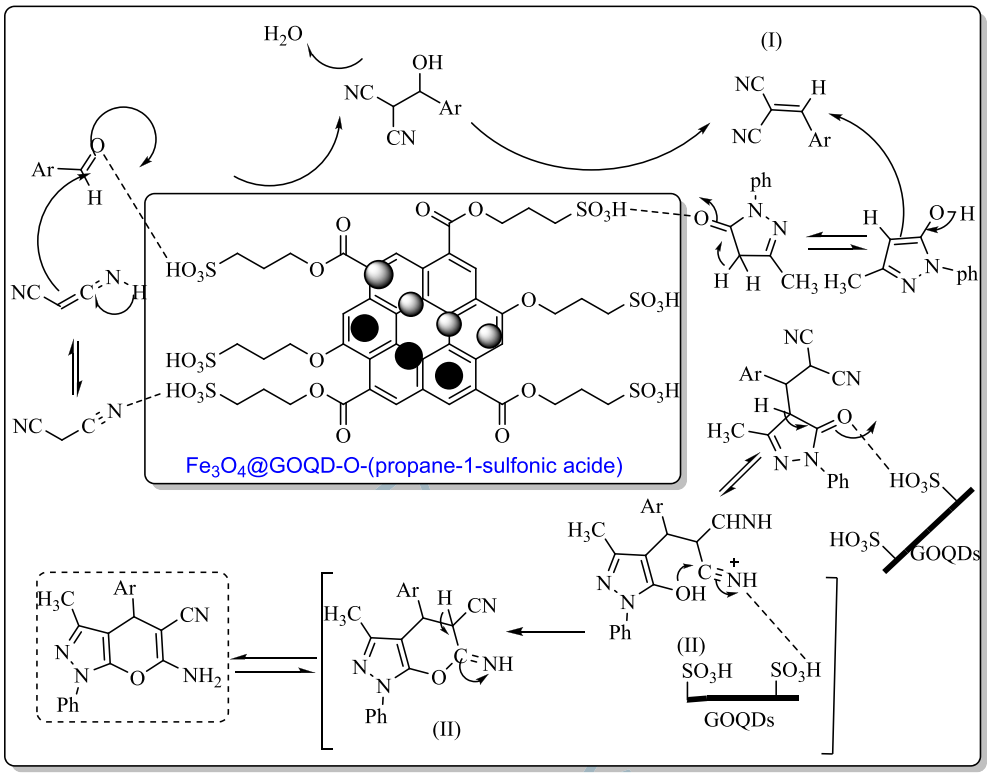

SCHEME 9 Possible mechanism for synthesis of 1,4-dihydropyrano[2,3-*c*] pyrazole derivatives catalysed by Fe_3O_4@GOQD-*O*-(propane-1-sulfonic acid)

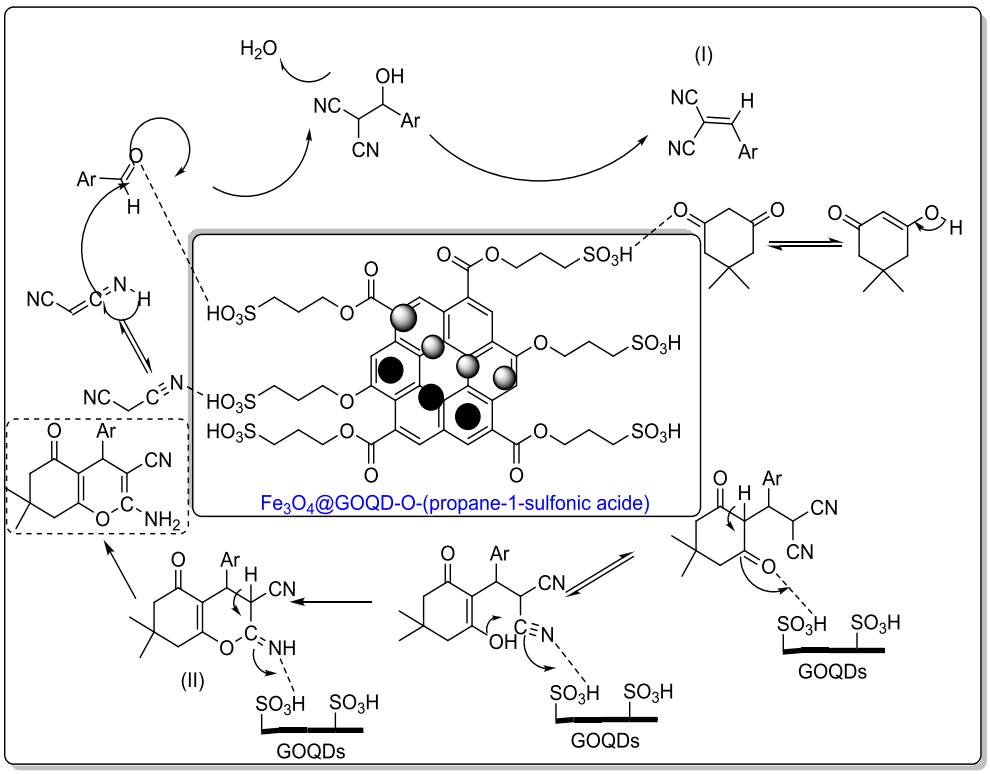

SCHEME 10 A possible mechanism for the synthesis of 2-amino-4-aryl-7,7-dimethyl-5-oxo-5,6,7,8-tetrahydro-4*H*-chromene-3-carbonitrile derivatives **4a**–**4h** catalysed by Fe_3O_4@GOQD-*O*-(propane-1-sulfonic acid)

aromatic aldehyde undergoes the electrophilic addition reaction with malononitrile under the catalytic effect of the acidic catalyst Fe_3O_4@GOQD-*O*-(propane-1-sulfonic acid) followed by dehydration to provide the 2-arylidenemalononitrile intermediate (**I**). In the next step, nucleophilic addition of 3-methyl-1-phenyl-2-pyrazolin-5-one to the intermediate (**I**) and intramolecular cyclization occur successively to yield the intermediate **II** which undergoes rearrangement to furnish the 1,4-dihydropyrano[2,3-*c*]pyrazol-5-yl cyanide derivatives **4a**–**4h**.

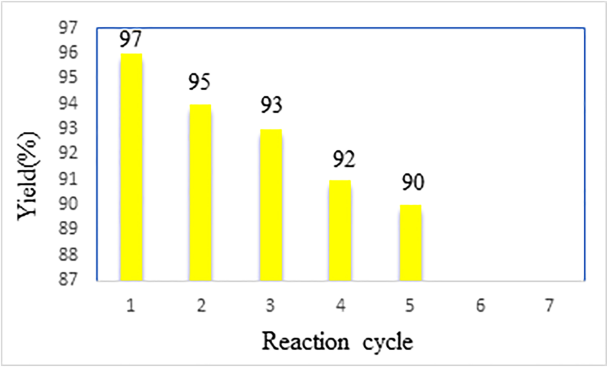

FIGURE 8 Recyclability of the catalyst Fe_3O_4@GOQD-*O*-(propane-1-sulfonic acid) for model synthesis of 2-amino-4-(*p*-nitrophenyl)-7,7-dimethyl-5-oxo-5,6,7,8-tetrahydro-4*H*-chromene-3-carbonitrile (**6g**)

A similar mechanism can be postulated for Fe_3O_4@GOQD-*O*-(propane-1-sulfonic acid)-catalysed three-component synthesis of 4*H*-chromene derivatives as depicted in Scheme 10. Similar to the mechanism shown in Scheme 9, in this mechanism too, condensation of the aldehyde with malononitrile takes place under the catalytic activation of Fe_3O_4@GOQD-*O*-(propane-1-sulfonic acid) to produce the arylidenemalononitrile intermediate (**I**) after dehydration. Subsequently, the catalyst-induced nucleophilic addition of the enolized dimedone to the intermediate (**I**) followed by consecutive intramolecular cyclization to provide the intermediate (**II**) which affords the expected 4*H*-chromenes **6a**–**6h** after rearrangement (Schemes 9 and 10).

4.4 | Catalyst recyclability

To examine the recyclability and stability of the catalyst Fe_3O_4@GOQD-*O*-(propane-1-sulfonic acid), we studied the model reaction between 4-nitrobenzaldehyde, dimedone and malononitrile under the optimized conditions. In order to examine the catalyst reusability, a hot filtration experiment was conducted and noticed that the reaction was completely stopped by removal of the solid catalyst. With regard to the hot filtration test and after

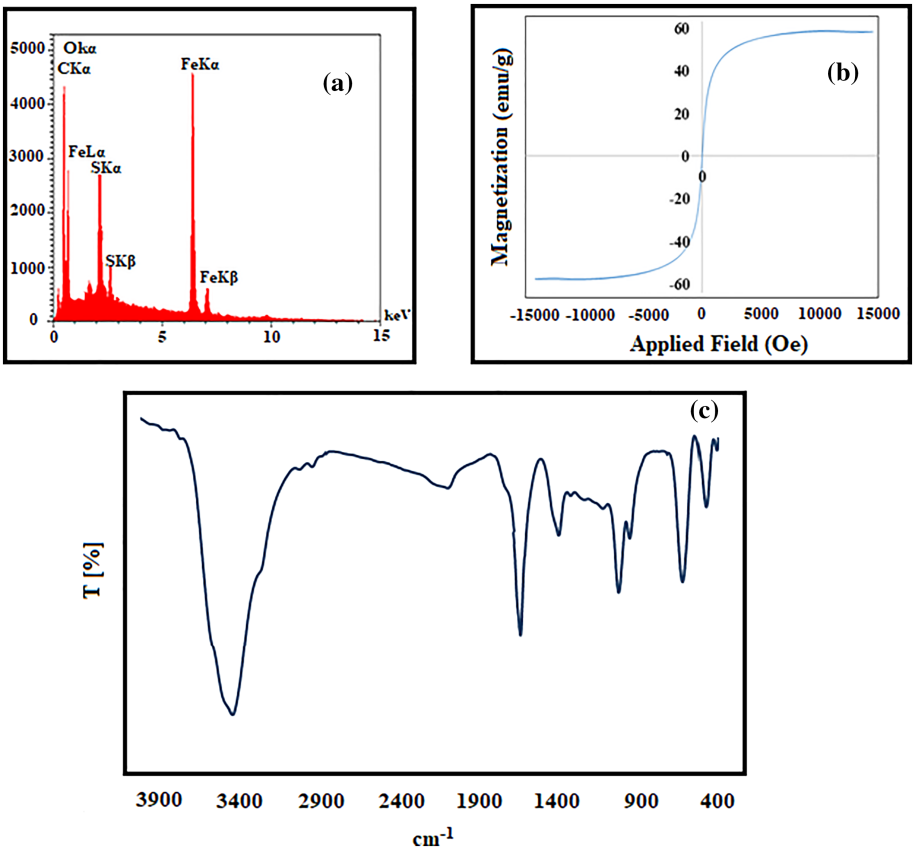

FIGURE 9 (a) The energy-dispersive X-ray (EDX) images of the catalyst after recycling, (b) vibrating sample magnetometer (VSM) image of the catalyst after recycling and (c) Fourier transform infrared (FT-IR) spectra for (Fe_3O_4@GOQD-*O*-(propane-1-sulfonic acid))

completion of the reaction, the magnetically isolated Fe_3O_4@GOQD-*O*-(propane-1-sulfonic acid) nanosheets were washed with hot EtOH/H_2O (1:1) several times, oven-dried at 65°C. As evidenced from Figure 8, the catalyst can be recycled and reused for at least five fresh runs without any significant loss of activity. The EDX, VSM, and FT-IR patterns were examined on the recycled catalyst and no significant changes were noticed on the recycled catalyst during the reaction and recovery process (Figure 9).

5 | CONCLUSIONS

In summary, we report in this research the successful fabrication of a novel hitherto unknown Fe_3O_4-magnetized propane-1-sulfonic acid-grafted GOQD (Fe_3O_4@GOQD-*O*-(propane-1-sulfonic acid)) nanocomposite film and its full characterization by FT-IR, EDX, SEM, XRD, TGA and VSM analytical techniques. The high catalytic performance of this newly prepared nanocomposite has been explored for one-pot synthesis of dihydropyrano[2,3-*c*]pyrazole and 4*H*-chromene derivatives. Use of water as a green solvent, simple reaction work-up, high reaction yields, low reaction times, easy magnetic separation of the catalyst from the reaction mixtures, efficient recyclability and reusability of the catalyst are the attractive features of the present protocol. On the basis of these advantages, the present method can be regarded as a convenient alternative for the synthesis of the titled heterocyclic compounds.

ACKNOWLEDGEMENTS

The Research Council of Bu-Ali Sina University and Islamic Azad University of Iran/North Tehran Branch are sincerely appreciated for technical support.

AUTHOR CONTRIBUTIONS

Masoud Khaleghi-Abbasabadi: Conceptualization; data curation; formal analysis; funding acquisition; investigation; methodology; project administration; resources; software; supervision; validation; visualization. **Davood Azarifar:** Conceptualization; data curation; formal analysis; funding acquisition; investigation; methodology; project administration; resources; software; supervision; validation; visualization. **Hamid Reza Esmaili Zand:** Conceptualization; data curation; formal analysis; investigation; methodology; resources; software; supervision; validation; visualization.

DATA AVAILABILITY STATEMENT

The data that supports the findings of this study are available in the supplementary material of this article.

ORCID

Masoud Khaleghi Abbasabadi https://orcid.org/0000-0002-1670-4542

Davood Azarifar https://orcid.org/0000-0002-7331-2748

REFERENCES

[1] G. A. Olah, A. Molnar, *Hydrocarbon Chemistry*, John Wiley Sons Inc **1995**.

[2] S. Wabg, Z. Wang, Z. Zha, *Dalton Trans.* **2009**, *43*, 9363.

[3] G. M. Scheuermann, L. Rumi, P. Steure, W. Bannwarth, R. Mulhaupt, *J.Am. Chem. Soc.* **2009**, *131*, 8262.

[4] N. R. Shiju, V. V. Guliants, *Appl Catal A-Gen.* **2009**, *356*, 1.

[5] (a)S. Dastkhoon, Z. Tavakoli, S. Khodabakhshi, M. Baghernejad, M. Khaleghi Abbasabadi, *N. J. Chem.* **2015**, *39*, 7268. (b)N. Koukabi, E. Kolvari, A. Khazaei, M. A. ZolFigol, B. S. Shaghasemi, H. R. Khavasi, *Chem. Commun.* **2011**, *47*, 9230. (c)D. Astruc, F. Lu, J. R. Aranzaes, *Angew. Chem. Inter. Ed.* **2005**, *44*, 7852. (d)M. V. Faraji, Y. V. Yamini, M. V. Rezaee, *J Iran Chem Soc.* **2010**, *7*, 1. eL. M. Rossi, N. J. S. Costa, F. P. Silva, R. V. Goncalves, *Nanotech Rev.* **2013**, *2*, 597. fS. J. Wang, Z. Y. Wang, Z. G. Zha, *Dalton Trans.* **2009**, *43*, 9363. gR. B. N. Baig, R. S. Varma, *Chem. Commun.* **2013**, *49*, 752.

[6] (a)A. Schatz, O. Reiser, W. J. Stark, *Chem. – Eur. J.* **2010**, *16*, 8950. (b)N. Yan, C. X. Xiao, Y. K. Coord, *Chem. Rev.* **2010**, *254*, 1179. (c)C. O. Dalaigh, S. A. Corr, Y. G. Ko, S. J. Connon, *Angew. Chem., Int. Ed.* **2007**, *46*, 4329. (d)F. Shi, M. K. Tse, M. M. Pohl, A. Bruckner, S. Zhang, M. Beller, *Angew. Chem., Int. Ed.* **2007**, *46*, 8866. (e)D. H. Zhang, G. D. Li, J. X. Li, J. S. Chen, *Chem. Commun.* **2008**, *29*, 3414. (f)M. R. Hoffman, S. T. Martin, W. D. Choi, W. Bahnemann, *Chem. Rev.* **1995**, *95*, 69. (g)A. Saxena, A. Kumar, S. Mozumdar, *J. Mol. Catal. A: Chem.* **2007**, *269*, 35. (h)A. T. Bell, *Science* **2003**, *299*, 1688. (i) S. Shylesh, J. Schweizer, S. Demeshko, V. Schunemann, S. Ernst, W. R. Thiela, *Adv. Synth. Catal.* **2009**, *351*, 1789.

[7] V. Polshettiwar, R. S. Varma, *Green Chem.* **2010**, *12*, 743.

[8] D. Guin, B. Baruwati, S. V. Manorama, *Org. Lett.* **2007**, *9*, 1419.

[9] (a)C. W. Lim, I. S. Lee, *Nano Today* **2010**, *5*, 412. (b)M. Zhang, Y. H. Liu, Z. R. Shang, H. C. Hu, Z. H. Zhang, *Catal. Commun.* **2017**, *88*, 39. (c)M. N. Chen, L. P. Mo, Z. S. Cui, Z. H. Zhang, *Curr. Opin. Green Sustain. Chem.* **2019**, *15*, 27.

[10] D. Azarifar, M. Khaleghi-Abbasabadi, *Res. Chem. Intermed.* **2019**, *45*, 2095.

[11] (a) S. Khodabakhshi, M. Khaleghi Abbasabadi, S. Heydarianc, S. Gharehzadeh Shirazi, F. Marahel, *Lett. Org. Chem.* **2015**, *12*, 465. https://doi.org/10.2174/1570178612666150331204620 (b) D. Azarifar, M. Khaleghi-Abbasabadi, *Res. Chem. Intermed.* **2019**, *45*, 199. (c)S. Shylesh, V. Schunemann, W. R. Thiel, *Am. Ethnol.* **2010**, *49*, 3428. (d)Y. H. Zhu, L. P. Stubbs, F. Ho, R. Z. Liu, C. P. Ship, J. A. Maguire, N. S. Hosmane, *ChemCatChem* **2010**, *2*, 365. (e)V. Polshettiwar, R. Luque, A. Fihri, H. B. Zhu, M. Bouhrara, J. M. Bassett, *Chem. Rev.* **2011**, *111*, 3036.

[12] (a)T. Q. Zeng, W. W. Chen, C. M. Cirtiu, A. Moores, G. H. Song, C. J. Li, *Green Chem.* **2010**, *12*, 570. bY. Zhang, C. G. Xia, *Appl. Catal. A.* **2009**, *366*, 141. cS. Laurent, D. Forge, M. Port, A. Roch, C. Robic, L. V. Elst, R. N. Muller, *Chem. Rev.* **2008**, *108*, 2064. dL. Ma'mani, M. Sheykhan, A. Heydari, M. Faraji, Y. Yamini, *Appl. Catal. A.* **2010**, *377*, 64. eB. Karimi,

E. Farhangi, *Chem. – Eur. J.* **2011**, *17*, 6056. fA. Rashidi, M. Khaleghi Abbasabadi, S. Khodabakhshi, *J Nat gas Sci Eng.* **2016**, *36*, 13. gA. Rashidi, Z. Tavakoli, Y. Tarak, S. Khodabakhshi, M. K. Abbasabadi, *J. Chin. Chem. Soc.* **2016**, *63*, 399. hM. Khaleghi Abbasabadi, A. Rashidi, J. Safaei-Ghomi, S. Khodabakhshi, R. Rahighi, *J. Sulfur Chem.* **2015**, *36*, 660. iM. Khaleghi Abbasabadi, A. Rashidi, S. Khodabakhshi, *J Nat gas Sci Eng.* **2016**, *28*, 87.

[13] (a)G. B. Dharma, M. P. Kaushik, A. K. Halve, *Tetrahedron Lett.* **2012**, *53*, 2741. (b)J. M. Khurana, K. Vij, *Tetrahedron Lett.* **2011**, *52*, 3666. (c)B. Karami, K. Eskandari, S. Khodabakhshi, *ARKIVOC* **2012**, *ix*, 76. (d)D. R. Dreyer, S. Park, C. W. Bielawski, R. S. Ruoff, *Chem. Soc. Rev.* **2010**, *39*, 228. (e) D. R. Dreyer, H. P. Jia, C. W. Bielawski, *Angew. Chem., Int. Ed.* **2010**, *49*, 6813. (f) S. Khodabakhshi, P. F. Fulvio, E. Andreoli, *Carbon* **2020**, *162*, 604. https://doi.org/10.1016/j.carbon.2020.02.058 (g)A. M. Rashidi, M. Mirzaeian, S. Khodabakhshi, *J Nat gas Sci Eng.* **2015**, *25*, 103.

[14] (a)K. S. Novoselov, Z. Jiang, Y. Zhang, S. V. Morozov, H. L. Stormer, U. Zeitler, J. C. Maan, G. S. Boebinger, P. Kim, A. K. Geim, *Science* **2007**, *315*, 1379. (b)M. Hosein Sayahi, S. Bahadorikhalili, S. J. Saghanezhad, M. A. Miller, M. Mahdavi, *Res. Chem. Intermed.* **2020**, *46*, 491. (c) S. F. Hojati, A. Amiri, E. Fardi, *Appl. Organomet. Chem.* **2020**, *34*. https://doi.org/10.1002/aoc.5604

[15] Y. Dong, C. Chen, X. Zheng, L. Gao, Z. Cui, H. Yang, C. Guo, Y. Chi, C. M. Li, *J. Mater. Chem.* **2012**, *22*, 8764.

[16] (a)X. Zhou, Y. Zhang, C. Wang, X. Wu, Y. Yang, B. Zheng, H. Wu, S. Guo, J. Zhang, *ACS Nano* **2012**, *6*, 6592. (b) D. Y. Pan, J. C. Zhang, Z. Li, M. H. Wu, *Adv. Mater.* **2010**, *22*, 734. (c)L. Tang, R. Ji, X. Cao, J. Lin, H. Jiang, X. Li, K. S. Teng, C. M. Luk, S. Zeng, J. Hao, S. P. Lau, *ACS Nano* **2012**, *6*, 5102. (d) S. Ahirwar, S. Mallick, D. Bahadur, *J. Solid State Chem.* **2020**. https://doi.org/10.1016/j.jssc.2019.121107 (e)S. Zhuo, M. Shao, S. T. Lee, *ACS Nano* **2012**, *6*, 1059. (f)S. Zhu, J. Zhang, S. Tang, C. Qiao, L. Wang, H. Wang, X. Liu, B. Li, Y. Li, W. Yu, X. Wang, H. Sun, B. Yang, *Adv. Funct. Mater.* **2012**, *22*, 4732. (g)H. Razmi, R. Mohammad-Rezaei, *Biosens. Bioelectron.* **2013**, *41*, 498. (h)V. Gupta, N. Chaudhary, R. Srivastava, G. D. Sharma, R. Bhardwaj, S. Chand, *J. Am. Chem. Soc.* **2011**, *133*, 9960. (i)H. Zhao, Y. Chang, M. Liu, S. Gao, H. Yu, X. Quan, *Chem. Commun.* **2013**, *49*, 234. (j) S. Zhu, J. Zhang, C. Qiao, S. Tang, Y. Li, W. Yuan, B. Li, L. Tian, F. Liu, R. Hu, H. Gao, H. Wei, H. Zhang, H. Sun, B. Yang, *Chem. Commun.* **2011**, *47*, 6858.

[17] J. L. Wang, D. Liu, Z. J. Zhang, S. Shan, X. Han, S. M. Srinivasula, C. M. Croce, E. S. Alnemri, Z. Huang, *Proc. Natl. Acad. Sci. U. S. a.* **2000**, *97*, 7124.

[18] C. B. Sangani, D. C. Mungra, M. P. Patel, R. G. Patel, *Chin. Chem. Lett.* **2012**, *23*, 57.

[19] A. K. Elziaty, O. E. A. Mostafa, E. A. El-Bordany, M. Nabil, H. M. F. Madkour, *Int. J. Sci. Eng. Res.* **2014**, *5*, 727.

[20] S. C. Kuo, L. J. Huang, H. Nakamura, *J. Med. Chem.* **1984**, *27*, 539.

[21] D. Azarifar, Y. Abbasi, *Synth. Commun.* **2016**, *46*, 745.

[22] (a)G. Vasuki, K. Kumaravel, *Tetrahedron Lett.* **2008**, *49*, 5636. (b)T. S. Jin, R. Q. Zhao, T. S. Li, *ARKIVOC* **2006**, *xi*, 176. (c) H. Sheibani, M. Babaie, *Synth. Commun.* **2010**, *40*, 257. (d) D. Azarifar, M. Tadayoni, M. Ghaemi, *Appl. Organomet. Chem.* **2018**, *32*, e4293. (e)M. S. Shingare, D. V. Mane, *Chin. Chem. Lett.* **2010**, *21*, 1175. (f)S. Gogoi, C. G. Zhao, *Tetrahedron Lett.* **2009**, *50*, 2252.

[23] (a)V. K. Tandon, M. Vaish, S. Jain, D. S. Bhakuni, R. C. Srimal, *Indian J. Pharm. Sci.* **1991**, *53*, 22. (b)L. Alvey, S. Prado, B. Saint-Joanis, S. Michel, M. Koch, S. T. Cole, F. Tillequin, Y. L. Janin, *Eur. J. Med. Chem.* **2009**, *44*, 2497. (c) H. Gourdeau, L. Leblond, B. Hamelin, C. Desputeau, K. Dong, I. Kianicka, D. Custeau, C. Boudreau, L. Geerts, S. X. Cai, J. Drewe, D. Labrecque, S. Kasibhatla, B. Tseng, *Mol. Cancer Ther.* **2004**, *3*, 1375. (d)T. Narender, S. Gupta Shweta, *Bioorg. Med. Chem. Lett.* **2004**, *14*, 3913. (e)M. Rueping, E. Sugiono, E. Merino, *Chem. – Eur. J.* **2008**, *14*, 6329. (f)M. T. Flavin, J. D. Rizzo, A. Khilevich, A. Kucherenko, A. K. Sheinkman, V. Vilaychack, L. Lin, W. Chen, E. M. Greenwood, T. Pengsuparp, J. M. Pezzuto, S. H. Hughes, T. M. Flavin, M. Cibulski, W. A. Boulanger, R. L. Shone, Z. Q. Xu, *J. Med. Chem.* **1996**, *39*, 1303. (g)M. Longobardi, A. Bargagna, E. Mariani, P. Schenone, S. Vitagliano, L. Stella, A. Di Sarno, E. Marmo, *Farmaco* **1990**, *45*, 399.

[24] J. M. Doshi, D. Tian, C. Xing, *J. Med. Chem.* **2006**, *49*, 7731.

[25] M. N. Erichsen, T. H. V. Huynh, B. Abrahamsen, J. F. Bastlund, C. Bundgaard, O. Monrad, A. Bekker-Jensen, C. W. Nielsen, K. Frydenvang, A. A. Jensen, L. Bunch, *J. Med. Chem.* **2010**, *53*, 7180.

[26] L. Bonsignore, G. Loy, D. Secci, A. Calignano, *Eur. J. Med. Chem.* **1993**, *28*, 517.

[27] S. J. Mohr, M. A. Chirigos, F. S. Fuhrman, J. W. Pryor, *Cancer Res.* **1975**, *35*, 3750.

[28] L. L. Andreani, E. Lapi, *Bull. Chim. Farm.* **1960**, *99*, 583.

[29] D. O. Moon, K. C. Kim, C. Y. Jin, M. H. Han, C. Park, K. J. Lee, Y. M. Park, Y. H. Choi, G. Y. Kim, *Int. Immunopharmacol.* **2007**, *7*, 222.

[30] Y. Peng, G. Song, *Catal. Commun.* **2007**, *8*, 111.

[31] (a)T. S. Jin, L. B. Liu, Y. Zhao, T. S. Li, *Synth. Commun.* **2005**, *35*, 1859. bL. M. Fotouhi, M. Heravi, A. Fatehi, K. Bakhtiari, *Tetrahedron Lett.* **2007**, *48*, 5379. cB. N. Seshu, N. Pasha, R. K. T. Venkateswara, P. P. S. N. Lingaiah, *Tetrahedron Lett.* **2008**, *49*, 2730. dF. Khorami, H. R. Shaterian, *Chin. J. Catal.* **2014**, *35*, 242. eN. M. A. bdEi-Rahman, A. A. Ei-Kateb, M. F. Mady, *Synth. Commun.* **2007**, *37*, 3961.

[32] W. S. J. Hummers, R. E. Offeman, *J. Am. Chem. Soc.* **1958**, *80*, 1339.

[33] Y. Shi, A. Pramanik, C. Tchounwou, F. Pedraza, R. A. Crouch, S. Reddy Chavva, A. Vangara, S. Sekhar Sinha, S. Jones, D. Sardar, C. Hawker, P. Chandra Ray, *ACS Appl. Mater. Interfaces* **2015**, *7*, 10935.

[34] M. Z. Kassaee, E. Motamedi, M. Majdi, *Chem. Eng. J.* **2011**, *172*, 540.

[35] S. B. Guo, S. X. Wang, J. T. Li, *Synth. Commun.* **2007**, *37*, 2111.

[36] L. G. Sharanina, V. K. Promonenkov, V. P. Marshtupa, A. V. Pashchenko, V. V. Puzanova, A. Y. Sharanin, N. A. Klyuev, L. F. Gusev, A. P. Gnatusina, *Chem. Heterocycl. Compd.* **1982**, *18*, 607.

[37] A. Saha, S. Payra, S. Banerjee, *Green Chem.* **2015**, *17*, 2859.

[38] M. Farahi, B. Karami, I. Sedighimehr, H. Mohamadi Tanuraghaj, *Chin. Chem. Lett.* **2014**, *25*, 1580.

[39] D. Azarifar, Y. Abbasi, O. Badalkhani, *J. Adv. Chem.* **2014**, *10*, 3197.

[40] D. Fang, H. B. Zhang, Z. L. Liu, *J. Hetrocycl. Chem.* **2010**, *47*, 63.
[41] S. Khaksar, A. Rouhollahpour, S. M. Talesh, *J. Fluorine Chem.* **2012**, *141*, 11.
[42] S. Balalaie, M. Bararjanian, M. Sheikh-Ahmadi, S. Hekmat, P. Salehi, *Synth. Commun.* **2007**, *37*, 1097.
[43] S. Sarrafi, E. Mehrasbi, A. Vahid, M. Tajbakhsh, *Chin. J. Catal.* **2012**, *33*, 1486.
[44] C. Nethravathi, M. Rajamathi, *Carbon* **2008**, *46*, 1994.
[45] G. Chen, S. Zhai, Y. Zhai, K. Zhang, Q. Yue, L. Wang, J. Zhao, H. Wang, J. Liu, J. Jia, *Biosens. Bioelectron.* **2011**, *26*, 3136.
[46] J. S. Wang, R. T. Peng, J. H. Yang, Y. C. Liu, X. J. Hu, *Carbohydr. Polym.* **2011**, *84*, 1169.
[47] X. J. Hu, Y. G. Liu, H. Wang, A. W. Chen, G. M. Zeng, S. M. Liu, Y. M. Guo, X. Hu, T. T. Li, Y. Q. Wang, L. Zhou, S. H. Liu, *Sep. Purif. Technol.* **2013**, *108*, 189.
[48] L. Z. Bai, D. L. Zhao, Y. Xu, J. M. Zhang, Y. L. Gao, L. Y. Zhao, J. T. Tang, *Mater. Lett.* **2012**, *68*, 399.
[49] S. Khodabakhshi, B. Karami, *New J. Chem.* **2014**, *38*, 3586.
[50] H. Kim, K. Y. Park, J. Hong, K. Kang, *Sci. Rep.* **2014**, *4*, 5278.
[51] C. Hou, Q. Zhang, M. Zhu, Y. Li, H. Wang, *Carbon* **2011**, *49*, 47.
[52] M. Mirza-Aghayan, M. Molaee Tavana, R. Boukherroub, *Ultrason. Sonochem.* **2016**, *29*, 371.
[53] P. Li, Y. Gao, Z. Sun, D. Chang, G. Gao, A. Dong, *Molecules* **2017**, *22*, 12.
[54] N. Far'aina, M. Mat Sallehb, M. Ashrafc, M. Y. Abd Rahmand, A. A. Umare, *Solid State Phenom.* **2017**, *268*, 259.
[55] K. V. Aken, L. Strekowski, L. Patiny, *Beilstein J. Org. Chem.* **2006**, *2*, 3.
[56] M. Abdollahi-Alibeik, A. Moaddeli, K. Masoomi, *RSC Adv.* **2015**, *5*, 74932.
[57] P. S. Sinija, K. Sreekumar, *RSC Adv.* **2015**, *5*, 101776.
[58] K. Niknam, N. Borazjani, R. Rashidian, A. Jamali, *Chin. J. Catal.* **2013**, *34*, 2245.
[59] A. Abdel Hamid, M. Abd-Elmonem, A. M. Hayallah, F. A. Abo Elsoud, K. U. Sadek, *Chem. Sel.* **2017**, *2*, 10689.
[60] M. Kangani, N. Hazeri, M. Taher Maghsoodlou, *J. Chin. Chem. Soc.* **2016**, *63*, 896.
[61] J. Yang, S. Liu, H. Hu, S. Ren, A. Ying, *Chin. J. Chem. Eng.* **2015**, *23*, 1416.
[62] A. A. Mohammadi, M. R. Asghariganjeh, A. Hadadzahmatkesh, *Arab. J. Chem.* **2017**, *10*, S2213.
[63] S. S. Pourpanah, S. M. Habibi-Khorassani, M. Shahraki, *Chin. J. Catal.* **2015**, *36*, 757.

SUPPORTING INFORMATION

Additional supporting information may be found online in the Supporting Information section at the end of this article.

How to cite this article: Khaleghi Abbasabadi M, Azarifar D, Esmaili Zand HR. Sulfonic acid-functionalized Fe_3O_4-supported magnetized graphene oxide quantum dots: A novel organic-inorganic nanocomposite as an efficient and recyclable nanocatalyst for the synthesis of dihydropyrano[2,3-*c*]pyrazole and 4*H*-chromene derivatives. *Appl Organomet Chem*. 2020;e6004. https://doi.org/10.1002/aoc.6004